Analysis of Key Safety Metrics of Thorium Utilization in LWRs

Brian Ade, Andrew Worrall, Jeffrey Powers, and Steve Bowman

Oak Ridge National Laboratory
PO Box 2008 MS6172
Oak Ridge, TN 37831-6172, adebj@ornl.gov

Abstract

Thorium has great potential to stretch nuclear fuel reserves due to its natural abundance and because it is possible to breed the ^{232}Th isotope into a fissile fuel (^{233}U). Various scenarios exist for utilization of thorium in the nuclear fuel cycle, including use in different nuclear reactor types (e.g., light water, high-temperature gas-cooled, fast spectrum sodium, molten salt), along with use in advanced accelerator-driven systems and even in fission-fusion hybrid systems. The most likely near-term application of thorium in the United States is in currently operating light water reactors (LWRs). This use is primarily based on concepts that mix thorium with uranium (UO_2 + ThO_2) or that add fertile thorium (ThO_2) fuel pins to typical LWR fuel assemblies. Utilization of mixed fuel assemblies (PuO_2 + ThO_2) is also possible.

The addition of thorium to currently operating LWRs would result in a number of different phenomenological impacts to the nuclear fuel. Thorium and its irradiation products have different nuclear characteristics from those of uranium and its irradiation products. ThO_2, alone or mixed with UO_2 fuel, leads to different chemical and physical properties of the fuel. These key reactor safety–related issues have been studied at Oak Ridge National Laboratory and documented in *Safety and Regulatory Issues of the Thorium Fuel Cycle* (NUREG/CR-7176, U.S. Nuclear Regulatory Commission, 2014).

This paper summarizes the analyses performed using the SCALE code system for comparison of key performance parameters of both ThO_2+UO_2 and ThO_2+PuO_2 against those of UO_2 and typical UO_2+PuO_2 mixed-oxide fuels, and includes the reactivity coefficients and power shares between surrounding UO_2 assemblies and the assembly of interest. The decay heat and radiological source terms for spent fuel after its discharge from the reactor are also presented. Based on this evaluation, potential impacts on safety requirements and identification of knowledge gaps that require additional analysis or research to develop a technical basis for the licensing of thorium fuel are identified.

Keywords: thorium, reactivity coefficients, decay heat

I. INTRODUCTION

Thorium (Th) has been widely considered an alternative to uranium (U) fuel throughout nuclear power history. Thorium has potential to stretch nuclear fuel reserves due to its natural abundance and because it is possible to breed the ^{232}Th isotope into a fissile fuel (^{233}U). Various scenarios exist for using thorium in the nuclear fuel cycle, including use in different nuclear reactor types (e.g., light water, high-temperature gas-cooled, fast spectrum sodium, molten salt), along with use in advanced accelerator-driven systems and even in fission-fusion hybrid systems. Different concepts also exist for recycling and reusing the fissile isotopes produced during irradiation of thorium fuel and the fertile isotopes that remain in the fuel.

The most likely near-term application of thorium in the United States is in currently operating light water reactors (LWRs). This use is primarily based on concepts that mix thorium with uranium (UO_2 + ThO_2), or concepts that add fertile thorium (ThO_2) fuel pins to typical LWR fuel assemblies. In addition, Thor Energy and Westinghouse have considered potential plans for testing PuO_2 + ThO_2) lead assemblies [1]. In general, it has been assumed that the fuel cladding and assembly design will remain identical to currently operating LWRs.

The addition of thorium to currently operating LWRs would result in a number of different phenomenological impacts to the nuclear fuel. Thorium and its irradiation products have different nuclear characteristics than those for uranium. In addition, ThO_2, alone or mixed with UO_2 fuel, leads to different chemical and physical properties of the fuel. These key reactor safety–related issues have been studied at Oak Ridge National Laboratory and documented in *Safety and Regulatory Issues of the Thorium Fuel Cycle* [2].

This paper summarizes reactor physics phenomena related to reactor safety using comparisons of thorium-fueled LWR design and operation requirements to those of the current uranium-fueled LWR fleet. Quantitative analyses have been performed, where practical, to estimate important trends and to confirm and illustrate the potential impact, significance, and magnitude of safety parameters of interest.

II. METHODOLOGY

In order to gain some basic understanding of the operating characteristics of thorium-based LWR fuels, a number of calculations were performed using the SCALE 6.1 [3–6] code system and ENDF/B-VII.0 cross section data. These calculations were for a typical LWR reactor fuel assembly, using four different fuel compositions. As a basis for comparison, results were generated for uranium oxide (UO_2, or UOX) and mixed oxide (UO_2 + PuO_2, or MOX). Equivalent fuel compositions were then generated for uranium/thorium oxide (UO_2 + ThO_2, or UTh) and plutonium/thorium oxide (PuO_2 + ThO_2, or PuTh). The terms “UTh” and “PuTh” are used as shorthand for these fuel mixtures; they are not indicative of chemical formulas. Thorium + ^{233}U mixed fuel has been omitted from these analyses for two reasons: (1) this research focuses on the mostly likely near-term utilization of thorium so utilization of ^{233}U as a fissile driver is unlikely in the near-term until sufficient ^{233}U is generated and recycled, and (2) this research focuses on the current fleet of LWR fuel and conversion to a full Thorium + ^{233}U cycle would likely require significant modification of the current LWR technology to be feasible.

One reference provided true equivalent fuel compositions for UOX (4.0 wt% ^{235}U/U) and MOX (8.0 wt% reactor-grade PuO_2) determined by full-core cycle analysis [7]. The 4.0 wt% ^{235}U/U UOX fuel was used as a basis for comparison of other fuel types throughout this study. Other literature suggested relevant fuel compositions for UTh and PuTh [8–14]; however, it was unclear

if the fuel compositions used in those studies were truly equivalent to 4.0 wt% ^{235}U/U UOX. True equivalent fuel compositions are typically determined by performing in-core fuel management and core design analysis with a full-core model. A simpler approach, the lifetime-average reactivity (LAR) method [7], was applied with an end-of-life (EOL) target of 48.5 GWd/MTHM in order to generate UTh and PuTh fuel compositions equivalent to the UOX and MOX fuel compositions determined from the literature survey [7]. In the LAR method, the reactivity of the model is integrated between beginning of life (BOL) and EOL and is then divided by the total burnup to give an "average" reactivity over the life of the fuel lattice. I.e., the LAR value of UOX is used as a reference, and then the other fuel initial compositions are adjusted such that the same LAR value is achieved given the same depletion conditions (soluble boron, moderator temperature, fuel temperature, etc.).

For the PuTh fuel, it was assumed that the plutonium isotopic vector in PuO_2 was identical to that used in the MOX fuel (reactor-grade plutonium) from Ref. 7. The PuO_2 and ThO_2 ratios were adjusted until the LAR matched that of UO_2, which yielded 9.0 wt% PuO2 with a balance of ThO_2.

For the UTh fuel, determination of the equivalent compositions was slightly more complicated. In the UTh fuel, there were two degrees of freedom: the fraction of UO_2 and ThO_2 and the ^{235}U enrichment. Excessively large fractions of UO_2 were required for low ^{235}U enrichments due to the increased capture of neutrons in thorium as compared to ^{238}U. For this reason, the ^{235}U fuel enrichment was increased to the maximum allowable for LEU (20.0 wt% ^{235}U) and the fraction of UO_2 and ThO_2 was adjusted until an acceptable fuel composition was found. The resulting fuel contained 26.0 wt% UO_2 and 74.0 $wt_{\%}$ ThO_2. The detailed fuel composition and final isotopic vector for each fuel type is listed in Table I.

A typical Westinghouse 17 × 17 (W17) pressurized water reactor (PWR) fuel assembly was chosen for this study [15]. A SCALE/TRITON [6] representation of the W17 model can be found in Figure 1. The four different "equivalent" fuel compositions (UOX, MOX, UTh, and PuTh) are listed in Table I. All fuel pins in the assembly consisted of the same composition (no radial zoning). In the depletion calculations, fuel compositions in each pin are tracked independently from all other fuel pins (i.e., a different composition is use for each fuel pin in the lattice). Further information regarding the process and reasoning behind the chosen fuel compositions, as well as other assumptions such as grid spacing and angular quadrature, can be found in Ref. 2.

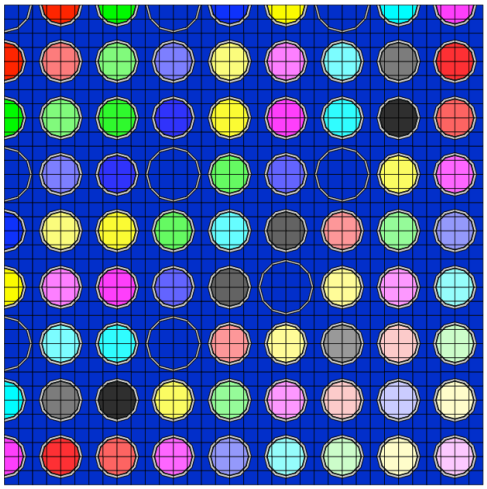

Figure 1. SCALE/TRITON representation of the ¼-W17 model.

Table I. Fuel composition summary

Isotope	UOX		MOX		PuTh		UTh	
	Element (wt %)	Fraction (%)*	Element (wt %)	Fraction (%)*	Element (wt %)	Fraction (%)*	Element (wt %)	Fraction (%)*
				UO_2				
^{234}U	0.035	100	0.002	92			0.199	26
^{235}U	4.000		0.300				20.000	
^{236}U	0.018		0.001				0.092	
^{238}U	95.947		99.697				79.709	
				PuO_2				
^{238}Pu			2.460	8	2.460	9		
^{239}Pu			54.690		54.690			
^{240}Pu			26.160		26.160			
^{241}Pu			9.510		9.510			
^{242}Pu			7.180		7.180			
				ThO_2				
^{232}Th			0.000		100.000	91	100.000	74

* Fraction of all heavy metal.

It was assumed that all fuel pins in the assembly model were of a single fuel type (i.e., all fuel pins contain only one of the four previously determined fuel compositions). Mixing of fuel pin types in a single lattice was not analyzed but could be a feasible design choice for thorium-bearing LWR fuel. It could be preferential to have thorium located along the edges of the fuel assembly, near guide tubes, or in some other location in the lattice for use in a seed-blanket configuration. In addition, no burnable absorbers (e.g., integral fuel burnable absorber, gadolinia, or wet annular burnable absorber) were used in the assemblies, although they are required in modern PWRs. The goal of the study was to determine preliminary operating characteristics of potential fuel types, not to generate an optimal fuel design or core-loading pattern using thorium.

Using the equivalent fuel compositions and the reference UOX and MOX fuel compositions, a number of different analyses were performed, which included reactivity coefficients (fuel temperature, moderator temperature, and boron), control rod reactivity, pin power peaking factors, and assembly power sharing. Analyses of out-of-reactor characteristics, such as decay heat and gamma spectra are also performed. In order to perform these analyses, the fuel assembly model in Figure 1 was depleted using the fuel compositions in Table 1 under typical PWR operating conditions [2]. The depleted fuel compositions were then extracted from the SCALE/TRITON output files at four different assembly-average burnup values: 0.0, 1.7, 25.1, and 48.5 GWd/MTHM, herein referred to as BOL, near beginning of life (NBOL), middle of life (MOL), and EOL. The fuel compositions corresponding to these burnup points were then used in single-state point calculations to determine various reactivity coefficients and other parameters of interest.

III. RESULTS

III.A. Reactivity Coefficients

A matrix of state conditions was developed for the reactivity coefficient calculations. Chosen volume-averaged fuel temperatures span 300 to 2400 K, which are expected to cover nominal, start-up, shutdown, and transient conditions. Four moderator temperatures between 566 and 614

K were used with corresponding moderator densities, which span nominal operating conditions. Lower moderator temperatures (e.g., 300 K) were considered but have been excluded from the case matrix, as the low temperatures are only likely during outage, start-up, and shutdown. Showing low moderator temperatures on the same plot as the operating temperatures (566 to 614 K) compresses the operating temperature range to a point where it is difficult to determine the overall trends. Four soluble boron concentrations ranging from 0 to 2400 ppm were chosen to span possible operating conditions from beginning of cycle (BOC) to end of cycle (EOC). In order to determine controlled lattice reactivity, calculations were performed for both "control rods in" and "control rods out" configurations (B_4C control rods were assumed). A summary of the state conditions for the reactivity coefficient case matrix is as follows:

- **Fuel temperature (T_f, K)**: 300, 900, 1200, 1500, 2100, and 2400
- **Moderator temperature (T_m, K)**: 566 (0.7426 g/cm^3), 583 (0.7073 g/cm^3), 600 (0.6641 g/cm^3), and 614 (0.6160 g/cm^3)
- **Soluble boron concentration (C_b, ppm)**: 0, 600, 1200, and 2400
- **Control rod state (CR):** out, in

Relevant data, including infinite multiplication factors and pin power distributions (peaking factors), were extracted from the SCALE/TRITON output files. The infinite multiplication factor data were used to generate reactivity coefficient plots over the range of conditions tested. A second-order polynomial was fitted to the k_{inf} data in order to smooth minor variations in the results that otherwise might lead to erroneous variations in the reactivity coefficient data. The derivative of the polynomial was then taken at various points to obtain the slope at those points. The slope of the k_{inf} curve represents the reactivity coefficient at that point. The change in reactivity has been calculated in percent mille (pcm or 1.0E-5), and reactivity coefficients, which represent the slope of the k_{inf} curve at that point, have been calculated as the change in reactivity divided by a change in a parameter of interest:

$$\Delta\rho = \frac{k_1 - k_2}{k_1 k_2} \; ; \; RTC = \frac{\Delta\rho}{P_1 - P_2}, \tag{1}$$

where

$\Delta\rho$ = the change in reactivity
k_n = the infinite multiplication factor for state $\underline{n}$
RTC = reactivity coefficient of interest
P_n = parameter of interest for state n

A set of base conditions is defined and used for depletion calculations, and then one of those base conditions (T_f, T_m, or C_b) is varied at a particular burnup point to generate the reactivity coefficient of interest. Fuel temperature reactivity coefficient (FTC, or Doppler coefficient) plots under normal PWR operating conditions (T_f = 900 K, T_m = 583 K, and C_b = 600 ppm) for BOL, NBOL, MOL, and EOL can be found in Figure 2. The FTCs for MOX and Th fuels are typically more negative than that of UOX for the selected state points. In PuTh and UTh fuels, the FTCs are considerably more negative than UOX and MOX. This characteristic is likely due to the presence of two large, temperature-sensitive capture resonances in ^{232}Th at ~20 and ~70 eV (indicated with blue vertical arrows), as seen in the ^{232}Th neutron capture cross section shown in Figure 3. The FTCs of all fuel types become more negative as the fuel burnup level increases.

The FTC for MOX is more negative than that of UOX due to the presence of strong thermal capture resonances in ^{239}Pu, ^{240}Pu, and ^{242}Pu. The BOL and EOL flux spectra for the four fuel types have been plotted in Figure 4. In addition to showing the impacts that large low-energy

thorium and plutonium resonances have on the flux spectra, Figure 4 indicates significant spectral-hardening effects resulting from the use of thorium and plutonium. UOX has the highest thermal neutron flux peak of the four fuels. Replacing some of the uranium in the fuel with thorium, as occurs when going from UOX to UTh fuel, results in a nearly 45% reduction of the thermal neutron flux. Both plutonium-bearing fuels (MOX and PuTh) exhibit nearly identical thermal neutron flux levels that are about 85% lower than for UOX and about 70% lower than for UTh. The lower thermal flux levels of MOX and PuTh fuels are accompanied by corresponding increases in fast flux levels. At fuel temperatures above 2000 K, the FTCs are similar for all fuel compositions because the harder spectra at higher fuel temperatures reduce the impact of the low-energy capture resonances in the Pu isotopes and ^{232}Th. The Doppler effect (Doppler broadening of resonances due to increase in temperature) in thermal reactors is primarily due to epithermal resonance absorption of neutrons for the non-fissile fuel isotopes in the studied fuel compositions (^{238}U, ^{240}Pu, and ^{232}Th). Because the FTC is sensitive to the fuel composition, it changes as a function of burnup. For example, in typical UOX fuel, the FTC becomes more negative as a function of depletion due to buildup of ^{240}Pu and other transuranic isotopes. All fuel compositions studied in this paper exhibit this behavior (i.e., more negative FTCs as a function of increasing burnup).

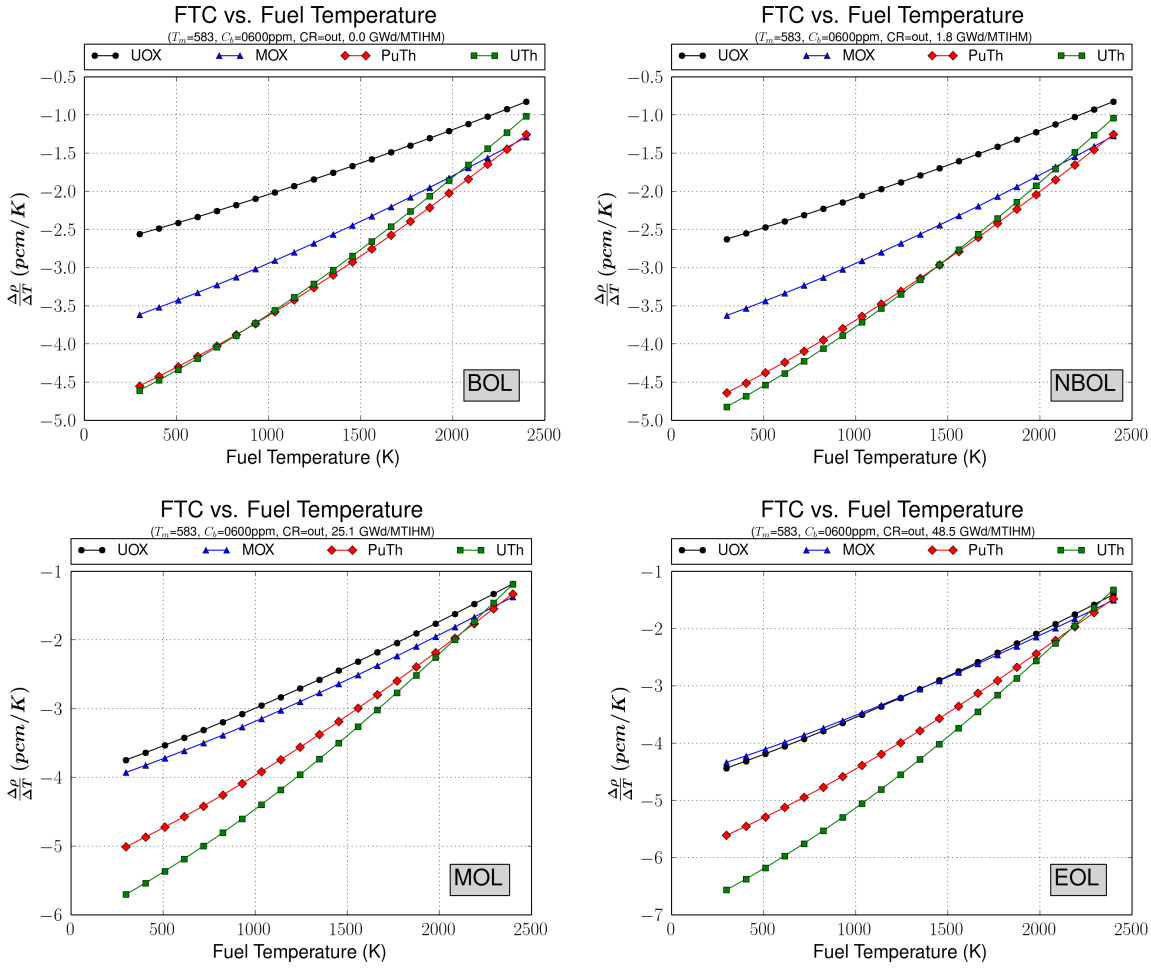

Figure 2. Fuel temperature coefficients of reactivity for BOL, NBOL, MOL, and EOL at T_m = 583 K and C_b = 600 ppm.

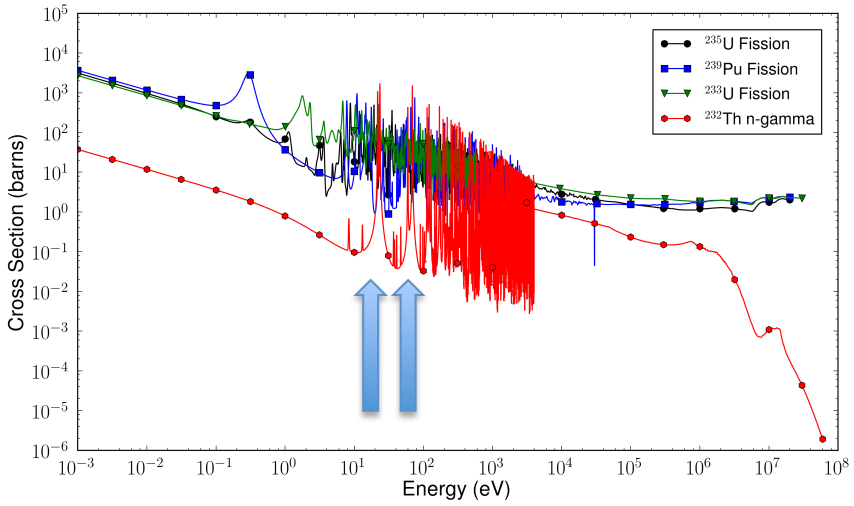

Figure 3. Selected neutron cross sections at 900 K.

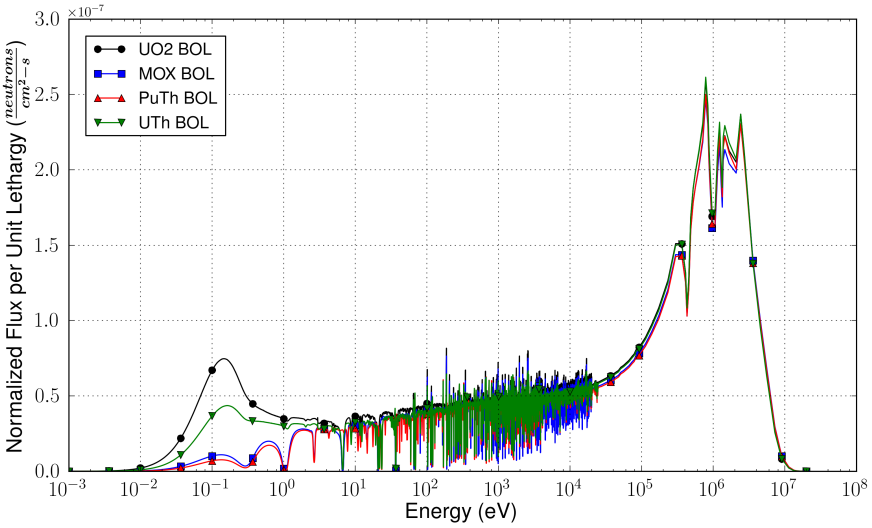

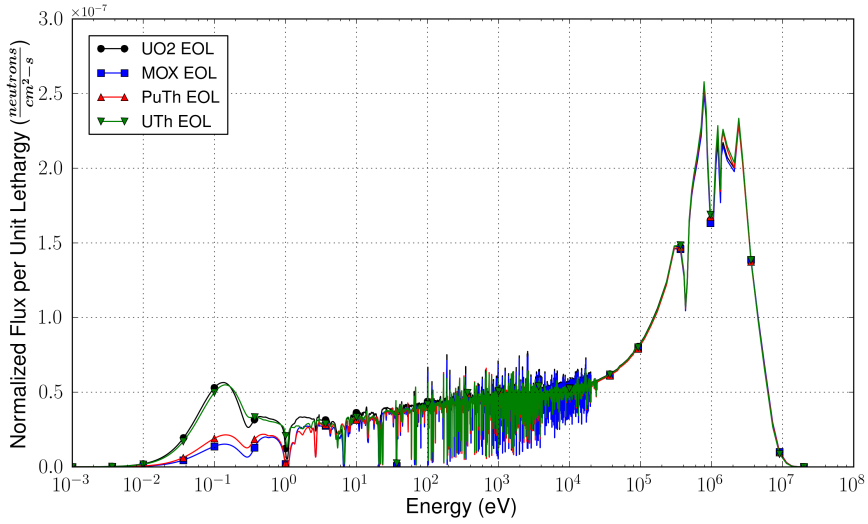

Figure 4. Normalized neutron spectra for UOX, MOX, PuTh, and UTh fuel at BOL (top) and EOL (bottom).

The fuel temperature and boron concentration were held constant to obtain the moderator temperature coefficient (MTC), shown in Figure 5. The MTCs for plutonium- and thorium-bearing fuels are more negative than for UOX at BOL and NBOL. An increase in moderator temperature leads to a decrease in moderator density, and thus a hardening of the neutron spectra. The harder neutron spectra result in increased neutron absorption in the resonance region, resulting in more negative MTCs. Due to the large low-energy capture resonances in plutonium, the MTCs for fuel types containing plutonium (MOX and PuTh) are more negative at lower burnups. However, the MTCs for PuTh and UTh become less negative than for UOX at EOL. This is primarily due to the softening of the neutron spectrum as a function of burnup for the thorium-bearing fuels. This spectral softening is exhibited in Figure 4, by comparing the BOL spectra (left) and EOL spectra (right) for UTh and PuTh fuel cases. The softening neutron spectrum as a function of increasing burnup is the opposite of that typically observed in LWRs using UOX fuel, leading to the rather significant change in moderator temperature coefficients over assembly life. In this study, no positive moderator temperature coefficients were calculated. Some studies have shown a far less negative moderator temperature coefficient for MOX fuel [10], primarily because of the increase in boron concentration that is needed in MOX-fueled reactors. In this study, the same boron concentration was used for all fuel cases, rather than adjusting the boron concentration to levels that would be needed for a particular type of core.

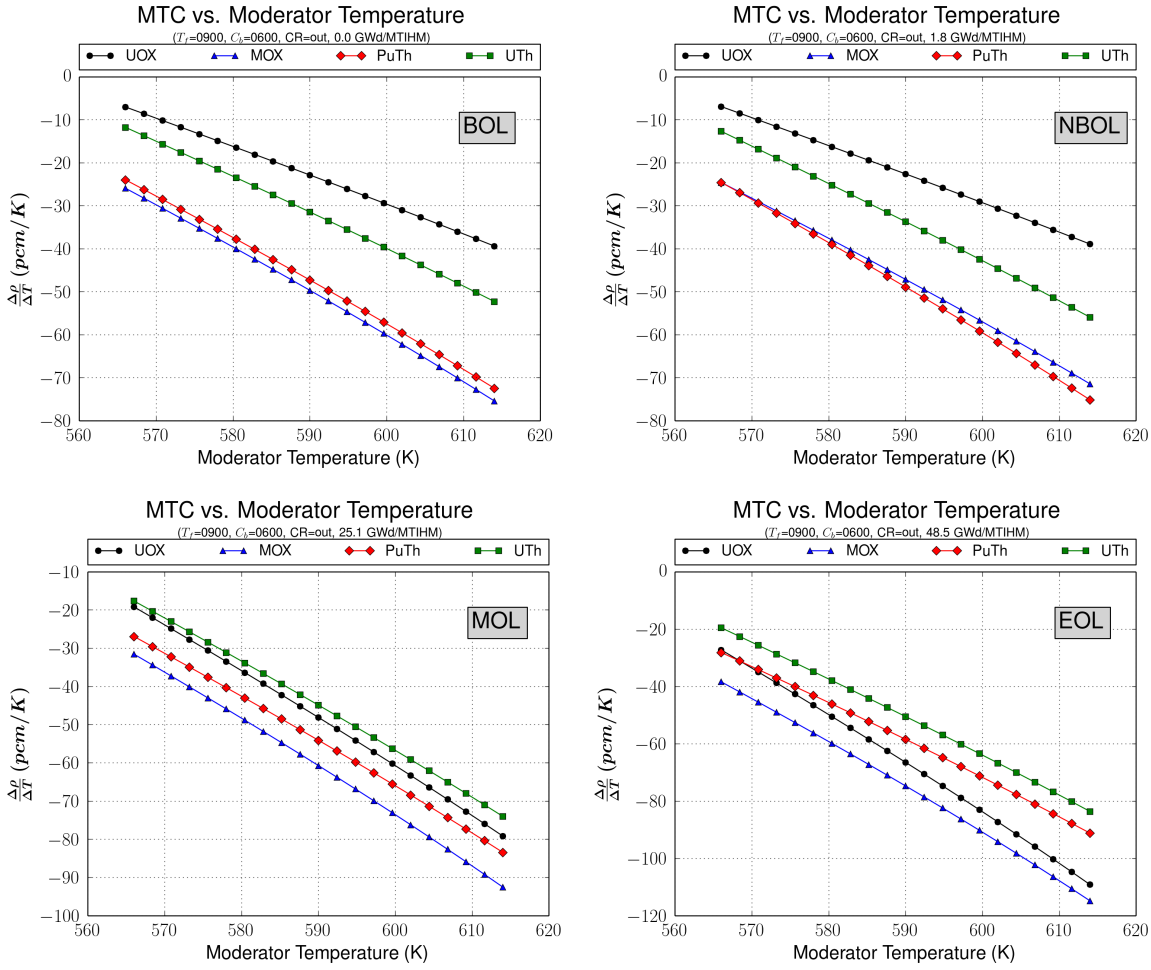

Figure 5. Moderator temperature coefficients of reactivity for BOL, NBOL, MOL, and EOL at T_f = 900 K and C_b = 600 ppm.

Similar plots and analyses were performed for boron concentration [2]; however, those plots have been omitted because they show no particularly interesting trends or surprises. In general, the boron worth in MOX and PuTh fuels is much lower than for UOX and UTh fuels, which leads to the need to increase boron concentrations or utilized enriched boron to maintain criticality and safety margins. The reactivity coefficient data are summarized in Table II. In general, for Th fuels, the Doppler coefficients and MTCs are more negative, which should increase safety margins. Conversely, the smaller boron worth for PuTh fuel could result in reduced effectiveness of boron-based safety systems and warrants further investigation.

Table II. Average reactivity coefficients over typical PWR conditions

Fuel type	Point in Life			
	BOL	**NBOL**	**MOL**	**EOL**
Average fuel temp. coeff., $300 \le T_f \le 2400$ (pcm/K)				
UOX	–1.74	–1.77	–2.54	–3.02
MOX	–2.53	–2.53	–2.73	–3.02
PuTh	–3.03	–3.08	–3.31	–3.71
UTh	–2.96	–3.09	–3.64	–4.18
Average moderator temp. coeff., $566 \le T_m \le 614$ (pcm/K)				
UOX	–23.01	–22.74	–48.50	–67.10
MOX	–50.04	–47.46	–61.19	–75.40
PuTh	–47.62	–49.25	–54.49	–58.91
UTh	–31.68	–33.94	–45.24	–50.91
Average boron coeff., $0 \le C_b \le 2400$ (pcm/ppm)				
UOX	–6.48	–6.35	–7.15	–8.67
MOX	–2.60	–2.58	–3.04	–3.64
PuTh	–2.69	–2.74	–3.25	–4.24
UTh	–5.81	–5.92	–6.59	–7.68

III.B. Control Rod Lattice Reactivity

The single-assembly models constructed for the reactivity coefficient test matrix were used to generate single-assembly control rod worths. Control rod worth is typically calculated using a full-core simulation, where the maximum rod worth for a certain core configuration can be obtained. In lieu of performing full core analyses, a subset of the input files used in the reactivity coefficient test matrix was modified to contain B_4C or AgInCd (AIC) control rods inserted into the guide tubes. These input files were then used to calculate the infinite multiplication factors, which were compared to the data generated for the unrodded conditions simulated in the reactivity coefficient test matrix (i.e., rods-in compared with rods-out). These calculations of infinite lattices at low burnups [infinite neutron multiplication factor (k-inf) >> 1] and high burnups (k-inf << 1) produce results that would differ from full core rod worth calculations where fuel assemblies with varying enrichments and burnups are loaded. In the future, additional studies using more robust full-core or more advanced 2-D methods are recommended to generate a more accurate representation of the rod worth.

The rod worth for BOL, MOL, and EOL burnup points is summarized in Table III for typical PWR operating conditions (T_f = 900 K, T_m = 583 K, and C_b = 600 ppm). For UOX, there is an increase in rod worth from BOL to EOL of approximately 15,000 pcm; the increase in rod worth for MOX, PuTh, and UTh is significantly less (~7,000–10,000 pcm). Comparing UOX and UTh, the average rod worth over the life of the assembly is similar (~45,000 pcm), but the addition of thorium to the fuel tends to slightly decrease the rod worth at EOL. The trend in rod worth for MOX and PuTh are very similar; the PuTh fuel having a slightly greater rod worth as a function of burnup. In all cases, the control rod worth increases as a function of increasing moderator temperature (and decreasing density), but the trend is strongest in UOX and UTh fuels.

There is little correlation between control rod worth and changing fuel temperature and changing boron concentration [2], so those results have been omitted. The trend of increasing control rod worth as a function of burnup is still observed for different fuel temperatures and boron concentrations, as well as the trend that the increase in control rod worth as a function of increasing burnup is larger for the fuels that contain uranium (UOX and UTh).

In order to determine the corresponding control rod worths for Ag-In-Cd (AIC) control rods, the B_4C used in previous calculations was replaced with AIC (80% Ag, 15% In, 5% Cd). The results for typical PWR conditions are compared to unrodded conditions to generate control rod worth for AIC control rods. The AIC results are summarized in the bottom portion of Table III. The control rod worths for AIC rods are lower than for B_4C rods, but the relative differences between traditional fuels (UOX and MOX) and thorium fuel types (PuTh and UTh) are very similar to the difference between B_4C rods and traditional rods. As with B_4C control rods, the AIC rod worth for UTh fuel type is approximately the same for UOX at BOL, but lower at EOL. The results for MOX and PuTh AIC control rod worth show similar trends as B_4C control rods. A nearly constant difference is observed as a function of burnup with the PuTh fuel having a slightly greater rod worth at each point.

Table III. Summary of single-assembly control rod worth

Point in Life	Rod worth (pcm × 10^3)			
	UOX	MOX	PuTh	UTh
	B_4C			
BOL	40	26	29	41
MOL	47	30	32	46
EOL	55	33	38	51
	AIC			
BOL	29	17	18	29
MOL	33	19	20	32
EOL	39	22	24	36

III.C. Pin Power Peaking and Power Sharing

For all cases in the reactivity coefficient test matrix, the pin power distributions were extracted and were used to determine the fuel pin peak power and peaking factors. The pin peaking factor is defined as the local pin power divided by the average pin power in the assembly, yielding a measure of the deviation of the pin power from the average in the assembly. Pin power distributions for T_f = 900 K, T_m = 583 K, and C_b = 600 ppm can be found in Figure 6 for BOL,

MOL, and EOL. As can be observed in Figure 6, the lattices containing plutonium result in higher power peaking near the guide tubes due to the increased thermal fission cross section of ^{239}Pu compared to that of ^{235}U. Generally, the fuels containing thorium result in slightly higher maximum pin-peaking factors than UOX or MOX (i.e., the pin peaking factors for UTh are higher than those for UOX, and the pin peaking factors for PuTh are higher than those for MOX). Although the differences are small, it could lead to a slight reduction in operating margins. The average (over all typical PWR conditions simulated) maximum pin peaking factor is 1.052 for UOX, 1.097 for MOX, 1.094 for PuTh, and 1.062 for UTh. Such small increases in pin peaking factors for thorium-bearing fuels is not expected to cause significant issues during reactor operation. In addition, it is likely these slightly higher peaking factors could be reduced through enrichment zoning and/or utilization of burnable poisons.

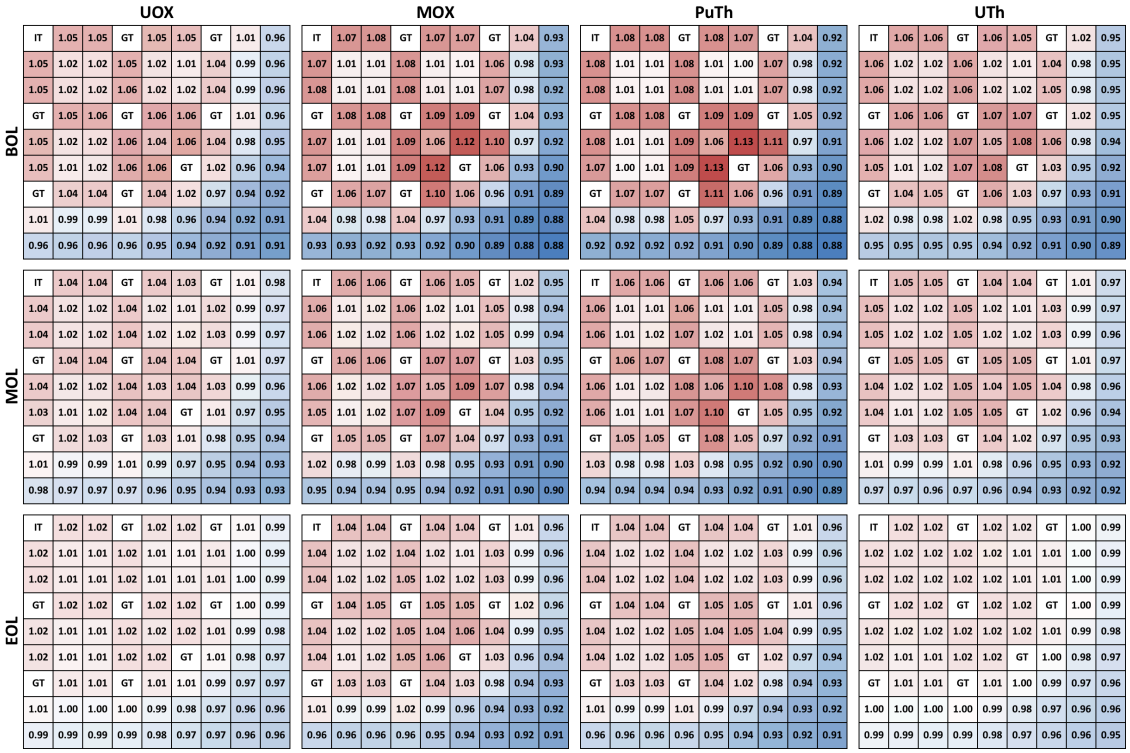

Figure 6. Pin power distribution for BOL, MOL, and EOL at T_f = 900 K, T_m = 583 K, and C_b = 600 ppm.

It is expected that a utility would initially choose to operate using a mixed-core of UOX fuel and some other fuel form. While the single assembly pin-peaking factors are useful, for a core of mixed fuel assemblies, single-assembly models are unlikely to accurately represent the realistic scenario. For this reason, additional calculations were performed using a 2×2 ¼-assembly array of fuel assemblies in a checkerboard pattern. In these cases, UOX fuel assemblies are always modeled as opposing corners of the array; the fuel compositions for the remaining assemblies are either UOX, MOX, UTh, or PuTh. These calculations have been performed at BOL, MOL, and EOL for each fuel type.

The results of these calculations for bundle power sharing can be found in Table IV. In Table IV, the three columns represent results for UOX at BOL, MOL, and EOL. The rows then represent all fuel types (UOX, MOX, UTh, or PuTh) at BOL, MOL, and EOL. The table presents the data in the format XX/YY [max peaking factor], where XX is the fractional power in the UOX reference

bundle (column headings), and YY is the power in the bundle of interest (row headings). The number in the brackets represent the maximum peaking factor of the two assemblies (i.e., the pin peaking factors for each bundle are calculated separately, and the maximum peaking factor of the values is placed in the brackets). The data in the table facilitate comparisons of a core containing only UOX with cores consisting of UOX/MOX, UOX/PuTh, and UOX/UTh. From the data in Table IV, it can be concluded that for nearly every case, the pin power peaking (noted in brackets in the table) increases when MOX or PuTh fuel assemblies are introduced. In some cases, the fuel bundle power sharing is actually flatter for the MOX and PuTh cases, but the peaking factor of the peak power pin is almost always greater. In order to mitigate these impacts, it is likely that some sort of burnable absorbers would be needed to reduce power peaking. For the UTh fuel, the fuel bundle power sharing and pin peaking are similar to the values observed for UOX-only models.

The true effect of the power sharing and the resulting power peaking (of assemblies and pins) could only be determined once a viable core design has been produced and full core analyses have been completed.

Table IV. Fuel bundle power sharing and highest peaking factor
Format: *XX*/*YY* [*ZZ*]*

Bundle of interest condition	UOX reference bundle condition		
	BOL	**MOL**	**EOL**
	UOX bundle of interest		
BOL	0.50/0.50 [1.06]	0.44/0.56 [1.22]	0.39/0.61 [1.36]
MOL	0.56/0.44 [1.22]	0.50/0.50 [1.04]	0.45/0.55 [1.17]
EOL	0.61/0.39 [1.36]	0.55/0.45 [1.17]	0.50/0.50 [1.02]
	MOX bundle of interest		
BOL	0.49/0.51 [1.19]	0.43/0.57 [1.26]	0.38/0.62 [1.35]
MOL	0.52/0.48 [1.25]	0.46/0.54 [1.21]	0.41/0.59 [1.32]
EOL	0.55/0.46 [1.32]	0.49/0.51 [1.17]	0.43/0.57 [1.27]
	PuTh bundle of interest		
BOL	0.50/0.50 [1.21]	0.45/0.55 [1.23]	0.39/0.61 [1.32]
MOL	0.53/0.47 [1.27]	0.47/0.53 [1.18]	0.42/0.58 [1.28]
EOL	0.56/0.44 [1.33]	0.50/0.50 [1.13]	0.45/0.55 [1.20]
	UTh bundle of interest		
BOL	0.51/0.49 [1.10]	0.45/0.55 [1.19]	0.40/0.60 [1.31]
MOL	0.54/0.46 [1.20]	0.49/0.51 [1.08]	0.43/0.57 [1.19]
EOL	0.58/0.42 [1.29]	0.52/0.48 [1.11]	0.47/0.53 [1.09]

**XX* = fraction power in the UOX reference bundle.
YY = power in the bundle of interest.
ZZ = maximum peaking factor.

III.D. Decay Heat

Decay heat characteristics play a significant role in both in-reactor and out-of-reactor safety analyses, so deviation from the prototypic UOX decay heat curves could have notable implications in accidents as well as medium- to long-term storage.

Previous research [2] revealed that the increase in ^{233}U concentration for thorium-bearing fuels reaches a point of diminishing returns after 60 GWd/MTHM (the rate of consumption of ^{233}U begins to balance production after that point). This result and the unknown fuel performance characteristics of very high burnup LWR fuel make it unlikely that the fuel will be used at very high burnups. In the analyses, 60 GWd/MTHM has been used as the maximum burnup. Burnup values of 25.1, 45.1, 60.2 GWd/MTHM have been used and are referred hereafter as low, typical (or normal), and high discharge burnup, respectively. More thorough analysis and results of the depleted fuel compositions and can be found in Ref. 2.

The total decay heat values for UOX, MOX, PuTh, and UTh for typical discharge burnup have been plotted in Figure 7 for decay times after discharge of up to 1000 years. The left plot in Figure 7 shows the full decay range; in the right plot, the timescale has been expanded to show data for decay times less than 1 year. Decay heat for the other discharge burnup values can be found in Ref. 2. The decay heat values for all fuels at times immediately after shutdown have the same order of magnitude. Figure 7 shows that of the fuel compositions utilized, fuels that initially contain uranium (UOX and UTh) follow the same general curve and that the fuels that initially contain plutonium (MOX and PuTh) follow a different decay heat curve. As expected, the decay heat increases as a function of increasing fuel burnup. Interestingly, the fuels that contain thorium (UTh and PuTh) have higher decay heat values than those that do not contain thorium (UOX and MOX) for decay times up to 0.3 years.

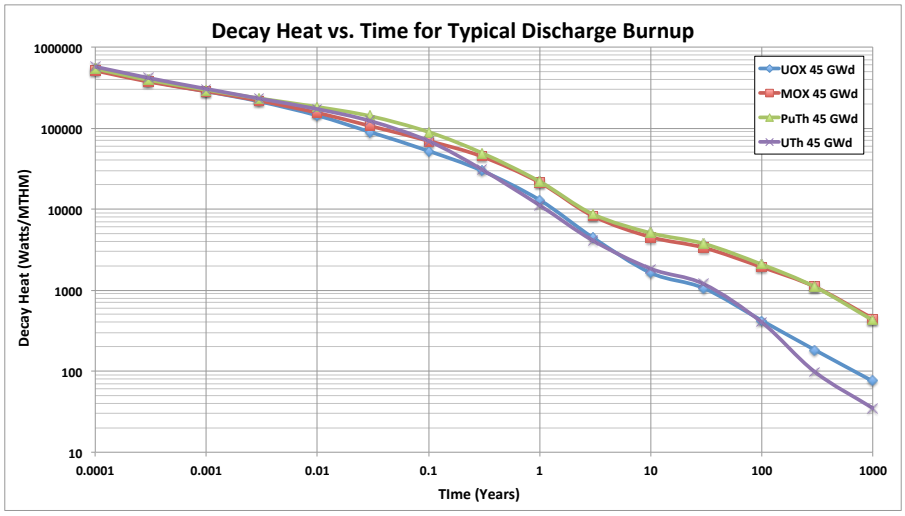

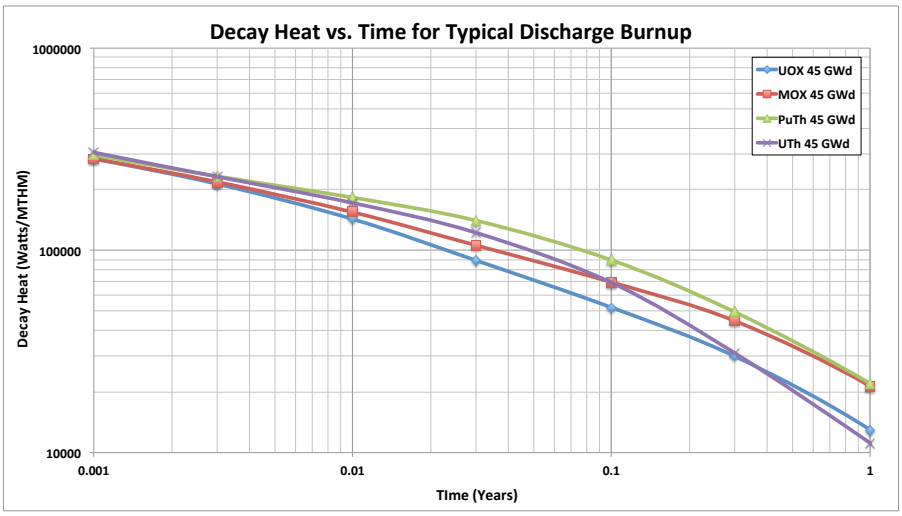

Figure 7. Decay heat as a function of decay time for typical burnup fuels.

The increase in decay heat up to 0.3 years could have implications for severe accidents, which can evolve over a number of days, and could also influence fuel-handling and core reloading maneuvers as well as storage in a spent fuel pool.

In order to further understand the main nuclides causing the decay heat differences for short decay times, the total decay heat of five nuclides that are the top contributors to the total decay heat at 0.1 years of decay have been plotted in Figure 8, for UOX (top) and UTh (bottom). Figure 8 shows that ^{233}Pa, which results from ^{232}Th neutron capture, is the largest contributor to decay heat for the first 0.1 years of decay for thorium fuel types. Although MOX and PuTh plots are not included here, it should be noted that ^{242}Cm is the largest contributor to decay heat for the first year of decay, for fuel types initially containing plutonium. In the case of PuTh fuel, the decay heat contribution of ^{233}Pa and ^{242}Cm is nearly equal after 0.1 years of decay [2].

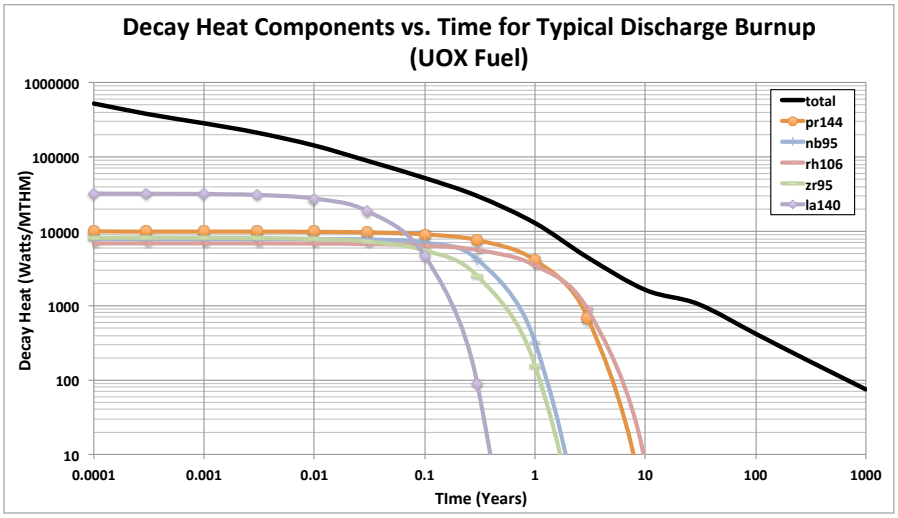

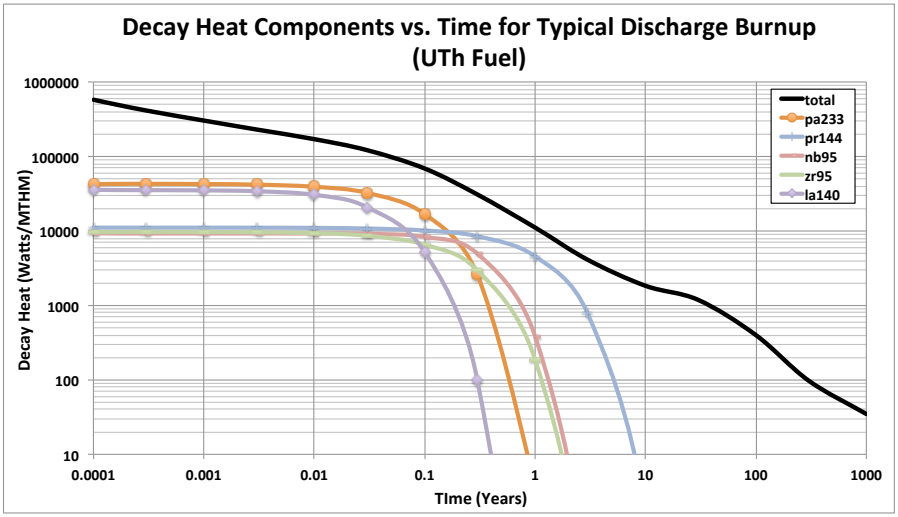

Figure 8. Decay heat components from top five contributing nuclides at 0.1 year of decay for UOX (top) and UTh (bottom).

The decay heat for each fuel type is summarized in Table V, which provides both the decay heat for each fuel type in kilowatts per metric ton of heavy metal and the ratio of the decay heat for a fuel type to that for typical UOX fuel. The data in the table indicate that immediately after shutdown (1 h decay time), the decay heat for the plutonium-bearing fuel types (MOX and PuTh) is slightly lower than for the uranium-based fuel types (UOX and UTh). At 1 month decay time, the UTh fuel decay heat is 25% higher than that of UOX, primarily due to ^{233}Pa, but is less than or similar to that of UOX for longer decay times. The Pu fuels have considerably larger decay heat values than UOX or UTh for decay times of 10 years or longer.

Table V. Summary of decay heat as a function of decay time

Fuel type	Decay time								
	1 hour	1 day	3 days	1 week	1 month	1 year	3 years	10 years	100 years
	Decay heat, W/MTHM								
UOX	517.4	222.2	160.7	118.2	61.60	12.93	4.457	1.631	0.419
MOX	506.3	229.1	171.4	132.3	78.81	21.24	8.247	4.513	1.913
PuTh	511.9	232.7	187.8	156.6	99.27	22.56	9.072	5.563	2.719
UTh	547.6	227.4	174.6	138.4	76.88	10.81	3.868	1.713	0.362
	Decay heat ratio*								
MOX/UOX	0.98	1.03	1.07	1.12	1.28	1.64	1.85	2.77	4.56
PuTh/UOX	0.99	1.05	1.17	1.32	1.61	1.74	2.04	3.41	6.48
UTh/UOX	1.06	1.02	1.09	1.17	1.25	0.84	0.87	1.05	0.86

*Ratio of selected decay heat with the decay heat of UOX fuel.

III.E. Gamma Spectra

The dominant pathway to ^{232}U is through the n-2n reaction in ^{232}Th, leading to 231Th, which then undergoes an beta decay, followed by an n-gamma, and another beta decay, leading to ^{232}U (~90% of ^{232}U). Additionally, the fertile isotope ^{232}Th undergoes neutron capture to become ^{233}Th, which after two successive beta decays, becomes the fissile isotope ^{233}U. ^{233}U will typically fission, but can also undergo an n-2n reaction, leading to production of ^{232}U (~10% of ^{232}U). Another minor pathway is found during the two successive beta decays from ^{233}Th to ^{233}U, ^{233}Pa (which has a 27 day half-life) can also undergo an n-2n reaction and becomes ^{232}Pa which then

beta decays to ^{232}U. Through these pathways, a relatively significant amount of ^{232}U is created during irradiation of ^{232}Th.

It is well known that the decay chain of ^{232}U contains substantial gamma emitters, the principal of those being ^{208}Tl. The ^{232}U nuclide decays to ^{228}Th with a half-life of 68.9 years, and then ^{228}Th decays to ^{224}Ra with a half-life of 1.9 years. The remaining decay chain is rather short lived and leads to ^{208}Tl, which emits four principal gamma rays. The highest yield gamma is the one with an energy of 2.62-MeV, which would cause significant shielding and handling concerns. In addition to ^{208}Tl, ^{212}Bi is also a gamma emitter with a number of medium- to high-energy gammas.

In order to illustrate the impact of the ^{232}U decay chain, the gamma spectra for the four fuel types have been plotted in Figure 9 using the 47-group BUGLE group structure [16]. The BUGLE group structure was originally developed for shielding calculations and is used as a typical gamma group structure for ORIGEN output. The gamma spectra were generated from the 45 GWd/MTHM burnup results, and have been plotted at a decay time of 30 years. Similar plots for additional decay times can be found in Ref. 2. In Figure 9, the gamma spectrum for the UTh fuel has been plotted over a decay time of 100 years, with the principal ^{208}Tl and ^{212}Bi gammas marked with vertical arrows. The height of each arrow corresponds to the gamma intensity of that particular isotope and energy.

Although an illustrating figure is omitted here for brevity, it should be noted that after 0.1 year (~30 days) of decay, the gamma spectra for all fuels are relatively similar, with the thorium-bearing fuels having some high-intensity, but low-energy gammas that could have an effect on handling of short cooling time irradiated thorium fuels. After 1 year of decay, the 2.62-MeV gamma from ^{208}Tl begins to appear clearly in the gamma spectra. After 30 and 100 years of decay, the impact of the 2.62-MeV gamma is very apparent, resulting in a very visible peak at that energy in the gamma spectra for PuTh and UTh fuels. These results indicate that additional shielding will likely be required for intermediate- and long-term handling and storage of thorium-bearing fuels.

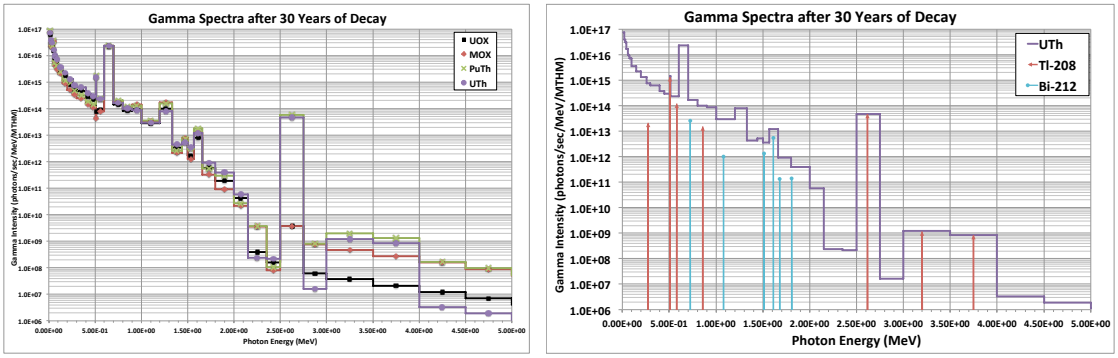

Figure 9. Forty-seven-group gamma spectra at 30 years decay time for the four tested fuel types (left) and for UTh with ^{208}Tl and ^{212}Bi gamma emission lines plotted (right).

IV. CONCLUSIONS

Steady-state and depletion analyses were performed using a two-dimensional Westinghouse 17 × 17 fuel assembly design to gain a basic understanding of the neutronic behavior of thorium-based fuels (UTh and PuTh) versus UOX and MOX fuels in current LWRs. The analyses included

reactivity coefficients, controlled lattice reactivity to estimate rod worth, and two-dimensional power peaking (fuel pins and assemblies).

The Doppler and moderator temperature coefficients for thorium-based fuels were generally more negative than those for UOX fuel, except for MTCs at EOL. For all simulated burnup points, the reactivity coefficient values were sufficiently negative to not have significant impacts on reactor operation. The UTh boron worth was approximately 1 pcm/ppm less negative than that for UOX fuel, which likely will have a minimal impact on LWR safety analyses, but further investigation would be needed to address the potential issue. The boron worth for the plutonium-bearing fuels (MOX and PuTh) was significantly less than for UOX and would certainly require additional safety analyses. This initial study indicates that the use of UTh fuel assemblies in LWRs is expected to have only a minor impact on lattice and core analyses. The behaviors of MOX and PuTh fuel assemblies appear to be similar to each other, but they show larger differences when compared to UOX fuel assemblies.

Using the spent fuel compositions obtained with the SCALE fuel assembly models from the in-reactor analyses, ORIGEN decay calculations were performed for low-, normal-, and high-discharge burnup values to determine decay heat and gamma spectra. The UTh fuel decay heat is 25% higher than that for UOX at 1 month of decay time after discharge, due to ^{233}Pa, but is less than or similar to UOX for longer decay times. The plutonium-bearing fuels have considerably larger decay heat values for decay times of 10 years or longer. In general, the fuels that initially contain uranium (UOX and UTh) exhibit the same type of variation for decay heat as a function of decay time. The fuels that initially contain plutonium (MOX and PuTh) follow a similar trend that is different from that of UOX or UTh up to ~30,000 years, after which, UTh and PuTh have higher decay heat than UOX and MOX [2]. The gamma spectra for fuel containing thorium are influenced by the gamma emitters in the decay chain of ^{232}U, namely ^{208}Tl. ^{208}Tl emits four principal gamma rays; the one with the highest yield is the 2.62 MeV gamma, which would cause significant shielding and handling concerns. At 0.1 year of decay time, the gamma spectra for all fuels are similar, however, PuTh and UTh have some relatively high intensity and low energy gamma emitters not present in UOX and MOX. After a 2-3 of years of decay time and beyond, the impact of the 2.62 MeV gamma results in a very visible peak in the gamma spectra for PuTh and UTh. These results indicate that additional shielding will likely be required for intermediate- and long-term handling and storage of thorium-based fuels.

The calculations documented herein represent a preliminary analysis of thorium-based fuels by way of comparison with conventional fuels. The results presented indicate the likely behavior for these fuel types; they do not provide a definitive statement of how they will perform. Full-core analyses would be needed to address assembly design optimization; core-loading pattern optimization; three-dimensional effects, including heterogeneity of fuel assembly burnup levels and heavy metal composition; and various other processes that could influence the results. Nevertheless, the results provide useful insight into some of the general trends and issues associated with comparison of the four fuel types studied and help identify possible safety and regulatory issues related to LWR thorium fuel cycles.

V. FUTURE WORK

The studies in this paper are meant to be only preliminary and further work on the subject is certainly warranted before utilization of thorium in currently operating LWRs. In the future, the determination of equivalent fuel compositions should be performed using a full-core model that takes into account phasing in thorium-based fuels, rather than using a

single lattice approach as has been done in the current work. A modern tool, such as VERA [15], being developed by CASL, would be an excellent choice for additional work in this area. Future work should also analyze the depletion of the fuel in greater detail, such as using radial rings and azimuthal regions to further ascertain the spatial depletion effects of thorium utilizations in LWRs. Additional and similar analysis could also be performed using the newly developed tools in SCALE 6.2 (to be released), such as Polaris, and the modern version of TRITON which both use a more refined cross section energy group structure [17].

Fuel cycle analysis and optimization has been omitted from this work; this work assumes that the thorium fuel cycle in LWRs make sense from fuel utilization and economics standpoints. Additional analysis should be performed to determine the fuel cycle advantages and disadvantages of thorium utilization in LWRs. The work could also be expanded to include other reactor types typically considered in thorium utilizations discussions, such as heavy-water reactors, molten-salt reactors, and various fast-reactor designs. Some of this research is being currently being performed by the U.S Department of Energy [9], and will inform future work in the area.

VI. ACKNOWLEDGEMENTS

The authors would like to thank the U.S. Nuclear Regulatory Commission and Mourad Aissa of the Office of Nuclear Regulatory Research for funding and providing guidance and feedback throughout this research. The authors would also like to thank ORNL staff members Germina Ilas and Matthew Francis for their thoughtful technical reviews, and Deborah Stevens and Walter Koncinski for technical editing.

References

1. J. Kelly and F. Franceschini, “Imminent: Irradiation Testing of (Th,Pu)O_2 Fuel,” Proceedings of Waste Management 2013, Phoenix, AZ, February 24–28.
2. B.J. Ade, A. Worrall, J. Powers, S. Bowman, G. Flanagan, and Jess Gehin, *Safety and Regulatory Issues of the Thorium Fuel Cycle*, NUREG/CR-7176, U.S. Nuclear Regulatory Commission, http://pbadupws.nrc.gov/docs/ML1405/ML14050A083.pdf.
3. *SCALE: A Comprehensive Modeling and Simulation Suite for Nuclear Safety Analysis and Design*, ORNL/TM-2005/39, Version 6.1.2 (February 28, 2013). (Available from Radiation Safety Information Computational Center at Oak Ridge National Laboratory as CCC-785.)
4. S. M. Bowman, "SCALE 6: Comprehensive Nuclear Safety Analysis Code System," *Nucl. Technol.* 174(2), 126-148, May 2011.
5. I. C. Gauld, G. Radulescu, G. Ilas, B. D. Murphy, M. L. Williams, and D. Wiarda, "Isotopic Depletion and Decay Methods and Analysis Capabilities in SCALE," *Nucl. Technol*. 174(2), 169–195, May 2011.
6. M.D. DeHart and S. M. Bowman, “Reactor Physics Methods and Analysis Capabilities in SCALE,” *Nucl. Technol.* 174(2), 196-213, May 2011.
7. A. Worrall, *Effect of Plutonium Vector on Core Wide Nuclear Design Parameters*, IAEA-SM-358/28, British Nuclear Fuels Limited, June 2000.

8. K. I. Bjork, C. W. Lau, H. Nylen, and U. Sandberg, "Study of Thorium-Plutonium Fuel for Possible Operating Cycle Extensions in PWRs" in *Science and Technology of Nuclear Installations*, Volume 2013, Article 867561, January 2013.
9. R. Wigeland, T. Taiwo, H. Ludewig, M. Todosow, W. Halsey, J. Gehin, R. Jubin, J. Buelt, S. Stockinger, K. Jenni, B. Oakley, *Nuclear Fuel Cycle Evaluation and Screening—Final Report: Appendix B, Comprehensive Set of Fuel Cycle Options*, Idaho National Laboratory Technical Report INL/EXT-14-31465 (2014).
10. H.R. Trellue, "Safety and Neutronics: A Comparison of MOX vs UO_2 Fuel," *Progress in Nuclear Energy*, 48, 135–145, 2006.
11. D. Yun, T.K. Kim, and T.A. Taiwo, *Th/U-233 Multi-Recycle in PWRs*, Argonne National Laboratory, prepared for the U.S. Department of Energy, ANL-FCRD-309, 2010.
12. M. Todosow, A. Galperin, S. Herring, M. Kazimi, T. Downar, and A. Morozov, "Use of Thorium in Light Water Reactors," *Nuclear Technology* 151, August 2005.
13. A. Galperin, E. Shwageraus, and M. Todosow, "Assessment of Homogenous Thorium/Uranium Fuel for Pressurized Water Reactors," *Nuclear Technology* 138(2), 111–122, May 2002.
14. G. Raites, M. Todosow, A. Galperin, and B. Gurion, "Non-Proliferation, Thorium-Based, Core and Fuel Cycle for Pressurized Water Reactors," Proceedings of ICONE-17, April 2012.
15. A. T. Godfrey, "VERA Core Physics Benchmark Progression Problem Specifications," CASL-U-2012-0131-002, Oak Ridge National Laboratory, March 2013.
16. "BUGLE-80: Coupled 47 Neutron, 20 Gamma-Ray Group, P3, Cross Section Library for LWR Shielding Calculations", by the ANS-6.1.2 Working Group on Multigroup Cross Sections", RSICC Data Library DLC-075.
17. M. A. Jessee, et. Al., "Polaris: A New Two-Dimensional Lattice Physics Analysis Capability for the SCALE Code System", Proceedings of PHYSOR 2014, Kyoto, Japan, September 28 - October 3, 2014.